Article

Syndiotactic Polystyrene Nanofibrils in Silica Nanotube Reactors: Understanding of Synthesis with Ultrahigh Molecular Weight

Kyu Yong Choi, Joong Jin Han, Bo He, and Sang Bok Lee

J. Am. Chem. Soc., **2008**, 130 (12), 3920-3926 • DOI: 10.1021/ja077272n

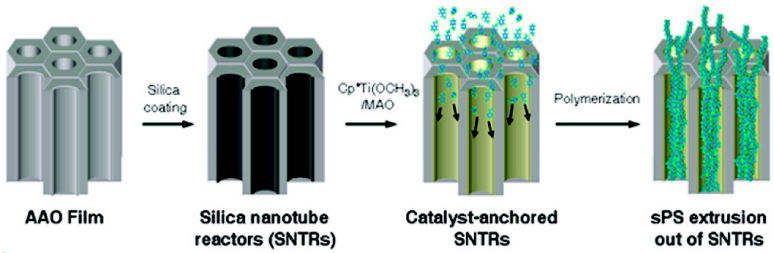

More About This Article

Additional resources and features associated with this article are available within the HTML version:

- Supporting Information
- Links to the 1 articles that cite this article, as of the time of this article download
- Access to high resolution figures
- Links to articles and content related to this article
- Copyright permission to reproduce figures and/or text from this article

View the Full Text HTML

J|A|C|S
ARTICLES
Published on Web 02/28/2008

Syndiotactic Polystyrene Nanofibrils in Silica Nanotube Reactors: Understanding of Synthesis with Ultrahigh Molecular Weight

Kyu Yong Choi,*,†,‡ Joong Jin Han,† Bo He,§ and Sang Bok Lee*,‡,§

Departments of Chemical and Biomolecular Engineering and Chemistry and Biochemistry and Maryland Nanocenter, University of Maryland, College Park, Maryland 20742

Received September 19, 2007; E-mail: choi@umd.edu; slee@umd.edu

Abstract: Nanofibrils of ultrahigh molecular weight syndiotactic polystyrene (sPS) have been synthesized in a silica nanotube reactor (SNTR) using a metallocene catalyst in conjunction with methylaluminoxane cocatalyst. Very thin sPS nanofibrils (<10 nm) grown at the catalytic sites on the pore walls aggregate to form intertwined, rope-like nanofibrils with 30−50 nm diameters, which further intertwine into even larger 200 nm diameter polymer nanofibrils. The extrusion of nanofibrils synthesized inside the SNTR was directly observed by scanning electron microscopy, and the individual SNTR containing a single polymer nanofibril was separated and observed by transmission electron microscopy. The sPS synthesized in the SNTR has ultrahigh molecular weight (M_w = 928 000 g/mol) with a large fraction of 2 000 000−5 000 000 g/mol molecular weight polymers.

Introduction

Syndiotactic polystyrene (sPS) is a new class of semicrystalline polymer with excellent chemical and physical properties (e.g., strong chemical resistance, high melting point (270 °C), low dielectric constant (2.5), and high crystallization rate) needed in harsh engineering applications in automotive, electrical, and electronics industries.[1,2] Both homogeneous and heterogeneous metallocene catalysts, mostly organometallic titanium complexes with methylaluminoxane (MAO) as an activator, have been found to be effective to synthesize sPS with high catalytic activity.[3−14] From an industrial point of view, it is desirable to heterogenize the catalyst by anchoring the catalyst onto a solid support and polymerize styrene in a liquid slurry polymerization process so that sPS can be obtained and easily treated as discrete particles.[2,15,16] The molecular weights (M_w) of sPS obtainable with heterogeneous catalysts are in the range 100 000−300 000 g/mol, and a molecular weight higher than 500 000 g/mol has not been reported. The effects of sPS molecular weight on the polymer properties are not well understood.[12] The synthesis of ultrahigh molecular weight polymers is of great industrial importance because such polymers may offer unusual properties, such as enhancement of mechanical strength, which is highly desirable in engineering polymers.

Recent advances in nanoscience and nanotechnology are opening new and interesting opportunities to synthesize polymers with unusual properties.[17−21] For example, very high electrical conductivity and high modulus of polymers synthesized in nanoscale pores have been reported.[17−19,21] The synthesis of ultrahigh molecular weight polymers in a confined nanoscale reaction environment is of interest, particularly in α-olefin polymerization with transition-metal catalysts. Most notably, Aida and co-workers used mesoporous silica fiber (MSF) with a pore diameter of 2.9 nm as a support for titanocene catalyst to polymerize ethylene.[22,23] The resulting polyethylene had a surprisingly high molecular weight ($>M_v$ = 6 000 000 g/mol) with the polymer nanofibrils extruding out from the mesopores of MSF, forming cocoon-like nanofiber bundles with

† Department of Chemical and Biomolecular Engineering.
‡ Maryland Nanocenter.
§ Department of Chemistry and Biochemistry.

(1) Malanga, M. *Adv. Mater.* **2000**, *12*, 1869−1872.
(2) Schellenberg, J.; Leder, H. J. *Adv. Polym. Technol.* **2006**, *25*, 141−151.
(3) Ishihara, N.; Seimiya, T.; Kuramoto, M.; Uoi, M. *Macromolecules* **1986**, *19*, 2464−2465.
(4) Ishihara, N.; Kuramoto, M.; Uoi, M. *Macromolecules* **1988**, *21*, 3356−3360.
(5) Ready, T. E.; Day, R. O.; Chien, J. C. W.; Rausch, M. D. *Macromolecules* **1993**, *26*, 5822−5823.
(6) Kaminsky, W.; Park, Y. W. *Macromol. Rapid Commun.* **1995**, *16*, 343−346.
(7) Po', R.; Cardi, N. *Prog. Polym. Sci.* **1996**, *21*, 47−88.
(8) Kaminsky, W.; Lenk, S. *Macromol. Symp.* **1997**, *118*, 45−54.
(9) Kaminsky, W.; Arrowsmith, D.; Strübel, C. *J. Polym. Sci., Part A: Polym. Chem.* **1999**, *37*, 2959−2968.
(10) Pellecchia, C.; Grassi, A. *Top. Catal.* **1999**, *7*, 125−132.
(11) Kim, Y.; Han, Y.; Do, Y. *J. Organomet. Chem.* **2001**, *634*, 19−24.
(12) Schellenberg, J.; Tomotsu, N. *Prog. Polym. Sci.* **2002**, *27*, 1925−1982.
(13) Qian, Y. L.; Zhang, H.; Zhou, J. X.; Zhao, W.; Sun, X. Q.; Huang, J. L. *J. Mol. Catal. A: Chem.* **2004**, *208*, 45−54.
(14) Huang, Q. G.; Chen, L. G.; Lin, S. G.; Wu, Q.; Zhu, F. M.; Shiyan Fu, Z. F.; Yang, W. T. *Polymer* **2006**, *47*, 767−773.
(15) Choi, K. Y.; Chung, J. S.; Woo, B. G.; Hong, M. H. *J. Appl. Polym. Sci.* **2003**, *88*, 2132−2137.
(16) Lee, H. W.; Chung, J. S.; Choi, K. Y. *Polymer* **2005**, *46*, 5032−5039.
(17) Menon, V. P.; Lei, J. T.; Martin, C. R. *Chem. Mater.* **1996**, *8*, 2382−2390.
(18) Demoustier-Champagne, S.; Stavaux, P. Y. *Chem. Mater.* **1999**, *11*, 829−834.
(19) Cepak, V. M.; Martin, C. R. *Chem. Mater.* **1999**, *11*, 1363−1367.
(20) Martin, C. R.; Kohli, P. *Nat. Rev. Drug Discovery* **2003**, *2*, 29−37.
(21) Arinstein, A.; Burman, M.; Gendelman, O.; Zussman, E. *Nat. Nanotechnol.* **2007**, *2*, 59−62.
(22) Lehmus, P.; Rieger, B. *Science* **1999**, *285*, 2081−2082.
(23) Kageyama, K.; Tamazawa, J.; Aida, T. *Science* **1999**, *285*, 2113−2115.

10.1021/ja077272n CCC: $40.75

Scheme 1. Synthesis of sPS Nanofibrils in Catalyst-Anchored Silica Nanotube Reactors

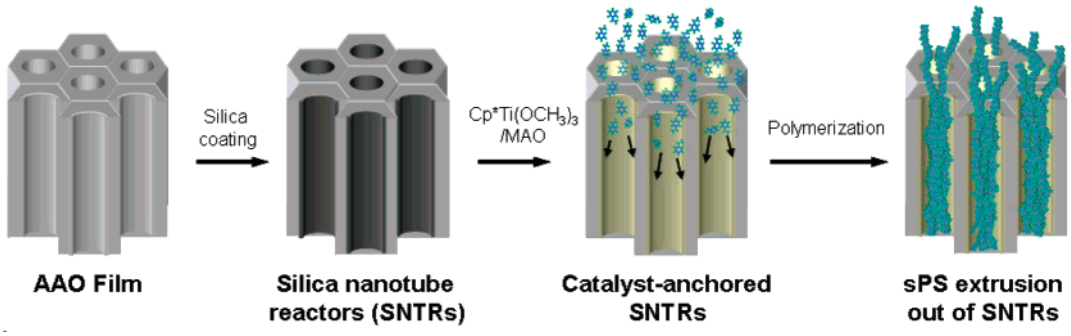

diameters of about 30−50 μm. The nanofiber bundles were comprised of ultrathin extended-chain crystal fibers 30−50 nm in diameter. Similar observations of polymer morphology were made by several other researchers with mesoporous silica.[24−26]

In spite of recent, intense interest in the synthesis and extrusion of polymers from a confined nanoscale reactor to investigate unusual polymer properties such as ultrahigh molecular weight and crystalline structure, an understanding of the polymer growth mechanism in the nanoscale reactor is still lacking. A challenging problem is that it is difficult to directly observe the resulting individual polymer nanofibrils after polymerization. The confined geometry in the nanoscale is expected to affect the polymerization reaction and produce some unusual physical properties, such as ultrahigh molecular weight and crystalline structures. However, the effects of confinement in the cases of polyethylene and polypropylene are inconsistent (e.g., some researchers report increased molecular weight, while some report no effect on molecular weight).[27,28] Several important factors appear to influence polymerization kinetics and polymer chain growth in the catalyst-anchored nanoscale pores: (i) physical factors, such as dispersion of catalyst on the pore surface, monomer and pore sizes, hindered diffusion of monomer into the pore, and restricted mobility of polymer chains or fibrils; and (ii) chain transfer reaction, such as β-hydride elimination, and chain transfer to monomer and aluminum alkyls that determine the polymer chain length.

In this paper, the extrusion of ultrahigh molecular weight sPS nanofibrils synthesized inside the SNTR was observed by scanning electron microscopy (SEM), and an individual SNTR containing a single polymer nanofibril was successfully separated and directly observed by transmission electron microscopy (TEM). A silica-coated nanoporous anodized aluminum oxide (AAO) film[29−32] was used as a polymerization reactor (we denote this as SNTRs, silica nanotube reactors or as an SNTR film). A metallocene catalyst (Cp*Ti$(OCH_3)_3$, pentamethylcyclopentadienyltitanium trimethoxide) was supported on the pores of a silica-coated nanoporous AAO film (Scheme 1). Such AAO films have several important advantages: (i) the film has well-defined nanoscale pores, and the pore length can be readily controlled; (ii) a metallocene/MAO catalyst complex can be effectively anchored onto a silica surface; (iii) the silica layer can be liberated from the AAO film as silica nanotubes containing sPS after polymerization, enabling a direct visual observation of polymer growth by transmission electron microscopy (TEM).

Experimental Methods

Materials. Pentamethylcyclopentadienyltitanium trimethoxide (Cp*Ti$(OCH_3)_3$, Strem Chemicals) was used with or without cocatalyst, methylaluminoxane (MAO, Albemarle, 10% in toluene, 4.55 wt % Al content). Styrene (Aldrich) was vacuum distilled over calcium hydride, and activated alumina was used to remove *tert*-butylcatechol (inhibitor) from the monomer. *n*-Heptane (Fisher Scientific), used as a diluent, was purified by being refluxed over sodium and benzophenone under a nitrogen atmosphere.

Silica Nanotube Reactor (SNTR). We used an anodized aluminum oxide (AAO) porous film as a basic frame for the nanotube reactor for styrene polymerization. The AAO porous film with 200 nm pores was purchased from Whatman, and the AAO films with smaller size pores (60 nm) were synthesized using the previously reported method.[31,32] The pore surfaces of these AAO films were coated with silica by the surface sol−gel (SSG) method: An AAO film was first soaked in $SiCl_4$ (99.8%) solution. It was then quickly immersed and washed with fresh hexane 4 times to remove unabsorbed $SiCl_4$. The top surface of the AAO film was gently polished mechanically, and the AAO film was placed in methanol/hexane (1:1 v/v) mixture and then ethanol before drying in nitrogen flow. Finally, the film was placed in a deionized water bath, followed by washing with methanol and a drying step. This procedure was repeated 5−10 times to obtain a 3−7 nm thick layer of silica at the pore surfaces.

Polymerization. To support metallocene catalyst onto the inner walls of a silica nanotube reactor, we used the same catalyst preparation technique used to make a silica-supported metallocene catalyst (anchoring catalyst on the surfaces of porous silica particles). To obtain high catalyst activity, an SNTR film was first treated with a MAO solution in toluene (7.5 vol %) at ambient temperature for 24 h, washed with toluene, and dried in vacuo. This treatment process was repeated twice. Then, the SNTR film was mixed with a Cp*Ti$(OCH_3)_3$ catalyst solution in toluene (0.013 mol/L) at ambient temperature for 24 h, washed with toluene, and dried in vacuo. The top and bottom surfaces of the SNTR film were mechanically polished to remove the catalyst exposed to the bulk liquid phase. To obtain low catalyst activity, the above catalyst anchoring procedure was used but without MAO treatment. For polymerization of styrene, the catalyst-deposited SNTR film was placed in a 20 mL glass bottle containing a liquid mixture of styrene and *n*-heptane. The concentration of styrene was varied from 2.5 to 5.0

(24) Tudor, J.; O'Hare, D. *Chem. Commun.* **1997**, 603−604.
(25) Tajima, K.; Ogawa, G.; Aida, T. *J. Polym. Sci., Part A: Polym. Chem.* **2000**, *38*, 4821−4825.
(26) Ye, Z. B.; Zhu, S. P.; Wang, W. J.; Alsyouri, H.; Lin, Y. S. *J. Polym. Sci., Part B: Polym. Phys.* **2003**, *41*, 2433−2443.
(27) Nakajima, H.; Yamada, K.; Iseki, Y.; Hosoda, S.; Hanai, A.; Oumi, Y.; Teranish, T.; Sano, T. *J. Polym. Sci., Part B: Polym. Phys.* **2003**, *41*, 3324−3332.
(28) Turunen, J. P. J.; Venäläinen, T.; Suvanto, S.; Pakkanen, T. T. *J. Polym. Sci., Part A: Polym. Chem.* **2007**, *45*, 4002−4012.
(29) Lee, S. B.; Mitchell, D. T.; Trofin, L.; Nevanen, T. K.; Soderlund, H.; Martin, C. R. *Science* **2002**, *296*, 2198−2200.
(30) Mitchell, D. T.; Lee, S. B.; Trofin, L.; Li, N. C.; Nevanen, T. K.; Soderlund, H.; Martin, C. R. *J. Am. Chem. Soc.* **2002**, *124*, 11864−11865.
(31) Son, S. J.; Reichel, J.; He, B.; Schuchman, M.; Lee, S. B. *J. Am. Chem. Soc.* **2005**, *127*, 7316−7317.
(32) Son, S. J.; Lee, S. B. *J. Am. Chem. Soc.* **2006**, *128*, 15974−15975.

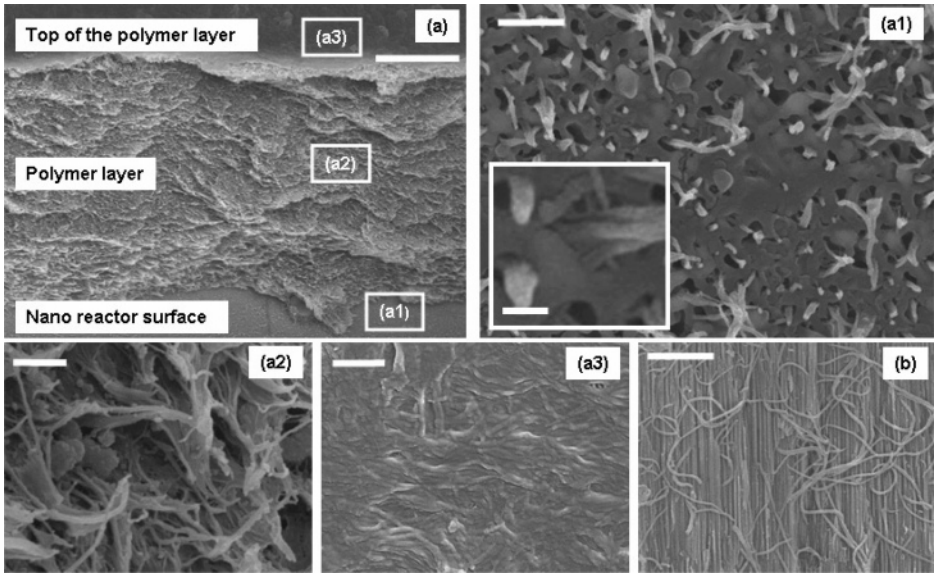

Figure 1. SEM images of sPS nanostructures: (a) vertical cross-section of the polymer layer on the SNTR film surface, (a1) top-down view of sPS nanofibrils extruded out from SNTR channels after the polymer layer was removed, (a2) sPS fibrils in the vertical cross-sectional view of the polymer layer, (a3) top-down view of the surface of the polymer layer, (b) vertical cross-section of the polymer-filled nanopore channels. Scale bars: (a) 20 μm, (a1−a3) 500 nm, inset of (a1) 100 nm, and (b) 5 μm.

mol/L, but the molecular weight of the polymer is little affected by the monomer concentration in this range.[33] The glass reaction bottle was placed in a constant temperature chamber. All experiments were carried out at 70 °C. The polymerization time was varied from 1 to 2 h for high-activity catalyst. For low-activity catalyst, polymerization was carried out for 8 h. After polymerization, the reaction mixture was removed from the bottle, washed with an excess amount of methanol, and then dried in vacuo.

Polymer Analysis. Dried SNTR/polymer samples were coated with a AuPd layer in a Denton DV-503 vacuum evaporator and analyzed by scanning electron microscopy (Hitachi S-4700). Transmission electron microscopic (TEM) analysis was carried out using a Zeiss EM10CA. ^{13}C nuclear magnetic resonance (NMR) spectrum was obtained at 90 °C with a Bruker 500 MHz DRX-500 spectrometer. The polymer solution was prepared by dissolving in 1,1,2,2-tetrachloroethane-d_2 (~1 mg/mL). The solvent peak was observed at 75 ppm. Differential scanning calorimetry (DSC) analysis was performed at a heating rate of 20 °C/min under nitrogen atmosphere using a Q1000 (TA Instruments). The molecular weights of sPS samples were measured by high-temperature gel permeation chromatography (PL GPC 220, Polymer Laboratories) with trichlorobenzene (TCB) at 160 °C. X-ray diffraction (XRD) analysis was performed using a Bruker D8 Advanced with GADDS (Bruker AXS).

Results and Discussion

In our first series of polymerization experiments, we used an SNTR film with a pore diameter of 200 nm. Figure 1a shows a vertical cross-sectional view of the fractured sample where a thick polymer layer (50−60 μm) covers the SNTR film surface. Here, polymer fibrils formed on the top surface of the silica-coated AAO film have been partially removed. Figure 1a1 shows a very revealing image of the SNTR film surface after removing the top polymer layer. In this figure the polymer nanofibrils can be seen coming out of the pores. The diameter of these sPS nanofibrils (30−50 nm) is smaller than the pore diameter, and it appears that the outlet of the 200 nm diameter pores is not completely filled with the polymer nanofibrils. In some pores, several sPS fibers of 30−50 nm are coming out independently or as a bundle (see inset in Figure 1a1). Figure 1a1 is direct evidence that sPS fibrils are formed inside the pores and extruded out to the bulk liquid phase.

A magnified image of the cross-section of the polymer layer is shown in Figure 1a2. The polymer layer consists of a massive amount of nanofibrils with 30−50 nm diameters. When the top surface of the polymer layer is also magnified as shown in Figure 1a3, the polymer layer consists of polymer nanofibrils with diameters of about 30−50 nm that are stacked on top of each other. These nanofibrils are stuck together as if they are partially fused. Figure 1b shows the vertical cross-section of the sPS-filled nanopore channels in the SNTR film below the polymer layer at the surface. It is seen that a large fraction of silica nanotubes is completely filled with long sPS nanofibrils, whereas some nanotubes are empty. This most likely occurs because the sPS nanofibrils are attached to the opposite side of the fractured SNTR channels. We also observed in Figure 1b that the diameters of the nanofibrils detached from the pores are very close to the pore diameter (200 nm).

The diameters of the sPS nanofibrils (30−50 nm) observed at the outlet of the SNTR film in Figure 1 are significantly smaller than the 200 nm diameter sPS nanofibrils observed inside the pores. The 30−50 nm sPS nanofibrils are quite similar to those observed in other geometrically confined catalytic polymerization systems. For example, when a mesoporous silica fiber or MCM-41 with a pore diameter of about 3 nm was used for ethylene polymerization with metallocene catalysts, polyethylene chains formed inside the mesopores aggregate into nanofibrils of about 30−50 nm as they exit from the mesopores.[22,23] These polyethylene nanofibrils aggregate further into polymer nanofibers of about 30−60 μm diameter. However, such a large diameter sPS nanofiber bundle was not observed in the current study. Recently, Kim and co-workers reported gas-phase ethylene polymerization in a bare AAO film deposited with a $TiCl_4/Al(C_2H_5)_3$ catalyst.[34] They observed the bundles of polyethylene nanofibers of 200 nm diameter and 3−5 μm

(33) Han, J. J.; Lee, H. W.; Yoon, W. J.; Choi, K. Y. *Polymer* **2007**, *48*, 6519−6531.

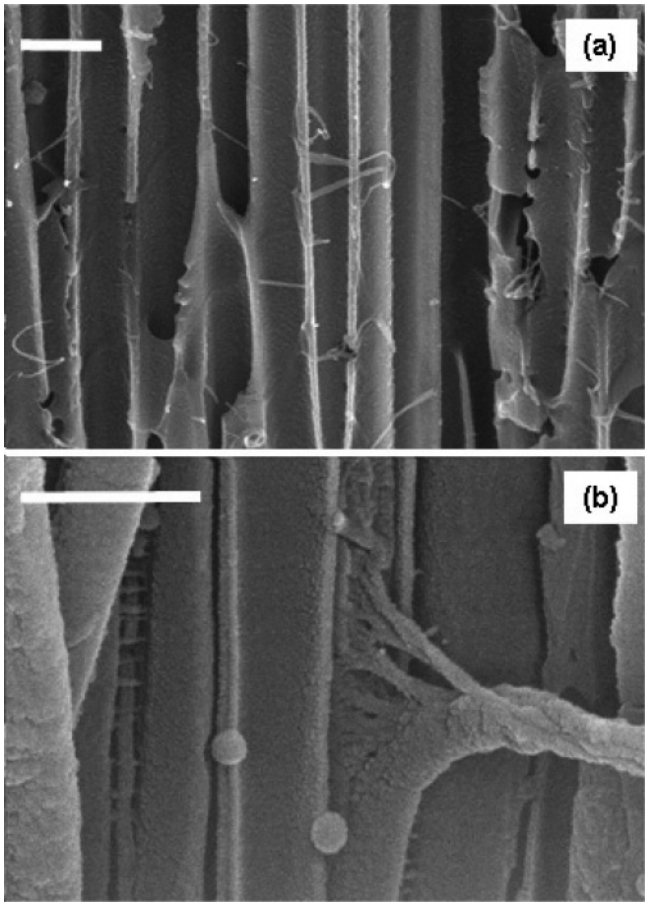

Figure 2. SEM images of sPS nanofibrils inside SNTR pores of diameter 200 nm: (a) low catalyst activity without MAO treatment and (b) high catalyst activity with MAO treatment. Scale bars: 500 nm.

length at the top surface of the AAO film and proposed that the polymer nanofibers were extruded out of the pores. Their experimental results indicate that polymerization occurred mostly near the inlet portion of the AAO film pores, forming a thick layer of polyethylene at the film surface. The nanochannels far from the pore entrance were mostly empty, and only small polymer dots and short fibers were observed.

To investigate the growth phenomena of sPS nanofibrils inside the 200 nm SNTR film, we carried out two polymerization experiments: one with and one without MAO cocatalyst. The low-activity polymerization without MAO enables us to observe the initial stage of fibrils growth. With high-activity polymerization with MAO, the later stage of nanofibrils growth can be observed. From the results shown in Figure 2, we propose a three-stage growth process of the nanofibrils as follows. The first stage involves formation of very thin nanofibrils, less than 10 nm in diameter (Figure 2a). In the second stage, these thin nanofibrils seem to aggregate by intertwining with each other to form a larger, rope-like cord. This newly formed structure has an approximately 50 nm diameter. In the third stage of growth, these larger nanofibrils again become intertwined to form an even larger nanofibril. In Figure 2b, which is the magnified view of the image shown in Figure 1b, the second-stage nanofibrils (coming off of the left side of the nanotube wall) are observed interconnecting and linking with each other in the third stage to form a larger nanofibril that is approximately 200 nm in diameter.

It is interesting that this final, large nanofibril is approximately the size of the SNTR pore itself: only one large nanofibril in each pore is seen in a vertical cross-sectional view of the SNTR nanopore (Figure 1b), but from a top-down view, multiple strands of sPS are seen extruding from each pore (Figure 1a1). The results shown in Figure 2b suggest that these multiple strands might be the second-stage nanofibrils that later intertwine to form the final, large nanofibril. Within the nanopore, movement of the second-stage nanofibrils can be restricted because of the increased tube pressure and minimal presence of liquid. Thus, these nanofibrils further intertwine into a large nanofibril. However, at the surface of the nanopore, the nanofibril exists in a liquid environment at a far lower pressure. Since there is ample room for the sPS nanofibril to spread out, this large, coiled nanofibril can then become loosened. The second-stage nanofibrils can separate from each other into multiple sPS strands, and we believe that this is the image that we see in Figure 1a1.

Growth of sPS nanofibrils inside the SNTR is further investigated using a 60 nm SNTR film with a smaller pore diameter (i.d. = 45 nm, o.d. = 60 nm) and a length of 5 μm. Figure 3 shows the resulting SEM images of the SNTR and the polymer fibers in the cross-section of the 60 nm silica nanotube reactor. Unlike the sPS sample analyzed in Figures 1 and 2, the 60 nm SNTR film in Figure 3 was fractured incompletely so that it was not vertically split through to the bottom. Instead, the membrane was split only $\sim$4 μm, as opposed to the full height of 5 μm. Fortunately, this cut enabled the film sides to split open, and both the vertical and horizontal cross-sectional areas could be viewed. Figure 3b shows the interior of the split-open SNTR. Notice that most of the silica nanotubes are filled with sPS nanofibrils. Some of these nanofibrils are detached from the reactor tube walls, but they remain connected to the tubes underneath. It is also seen that some of these nanofibrils are cut and hung loose between the top and bottom pieces of the film. Figure 3c is the magnified image of the horizontal cross-section. Notice that some of the nanofibrils inside the silica nanotubes are still connected to the side wall of the fractured reactor tube surfaces. Also, only one polymer nanofibril is filling each of the 60 nm nanotubes. Recall that in Figure 1 for the 200 nm SNTR multiple sPS fibrils were present in the tubes.

The sPS nanofibrils were directly observed inside the 60 nm silica nanotubes (SNTs) by TEM. The top of the 60 nm SNTR film was mechanically polished to remove the polymer layer that was extruded out from the pores of silica nanotubes and deposited on the top surface. The silica nanotubes containing sPS were liberated after dissolving alumina selectively in a 0.1 M NaOH solution and then collected by filtration. Figure 4a shows the TEM images of the nanotubes containing sPS. Each silica nanotube is partially filled with a single sPS nanofibril whose diameter is smaller than the pore diameter. Since the inner pore diameter is only 45 nm, the sPS nanofibrils cannot intertwine into larger fibrils that were observed in Figure 2b as the third-stage nanofibrils. Figure 4b shows the pieces of broken silica nanotubes. Inside a broken silica nanotube, the sPS polymer remains unbroken but bent with the same angle as the silica tube. It is quite interesting to observe that the sizes of the sPS nanofibrils are nearly constant along the tube length. This

(34) Nair, S.; Naredi, P.; Kim, S. H. *J. Phys. Chem. B* **2005**, *109*, 12491−12497.

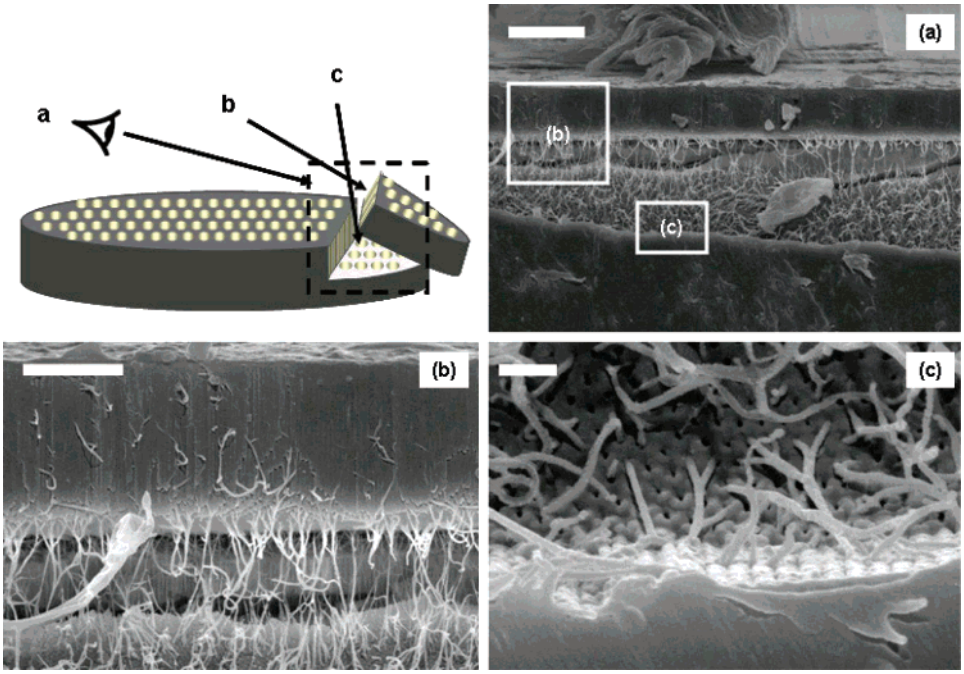

Figure 3. SEM images of sPS nanostructures synthesized in a 60 nm SNTR film: (a) vertical cross-section of the SNTR film, pore diameter = 60 nm and (b, c) magnified images. The cartoon in the top-left corner illustrates the viewing angles for the images (a−c). The polymer layer on the SNTR film and the sPS nanofibrils are omitted for clarity. Scale bars: (a) 5 μm, (b) 2 μm, and (c) 250 nm.

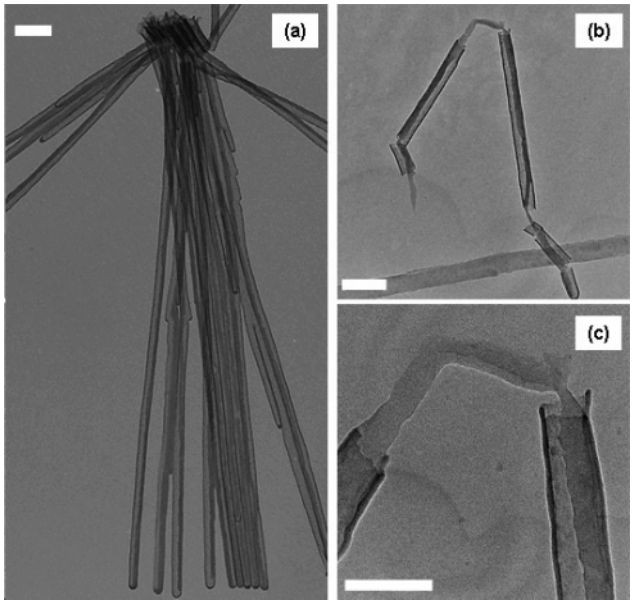

Figure 4. Transmission electron micrographs (TEM) of 60 nm diameter silica nanotubes containing sPS polymerized at the inner surface of the pore walls. Scale bars: (a and b) 250 and (c) 100 nm.

suggests that the polymerization reaction occurred uniformly throughout the interior of SNTR nanochannel, which implies that the catalysts are anchored well and homogeneously active throughout the SNTR channels. Figure 4c shows a high-resolution TEM image of the exposed area of a sPS nanofibril out of the broken silica nanotube in Figure 4b.

The synthesized nanofibrils were analyzed by ^{13}C NMR spectroscopy (Figure 5a). The characteristic peak at 145.5 ppm confirms that the polymer fibrils obtained are syndiotactic polystyrene, and the entire spectrum matches very well with those of sPS in previous reports.[3,35] The syndiotacticity of the polymer fibrils measured by the ^{13}C NMR is 100% (i.e., single peak at 44.3 ppm in the 43.0−47.0 ppm range). Molecular weight and molecular weight distribution (MWD) are important polymer parameters that have a significant impact on the polymer's physical, mechanical, and rheological properties. Figure 5b shows two MWD curves of the sPS polymerized using the silica nanotube reactor and the silica-supported Cp*Ti-$(OCH_3)_3$ catalyst at 70 °C. Here, a striking difference between the two sPS samples is observed: the sPS produced in the SNTR has a molecular weight (M_w = 928 000 g/mol) which is 4.2 times larger than the molecular weight of the sPS obtained using silica-supported catalyst at higher monomer concentration (M_w = 221 000 g/mol). In the MWD curve for the SNTR polymer, we observe that about 40 wt % of sPS has a molecular weight larger than 1 000 000 g/mol. The largest molecular weight detected in the MWD curve is very close to 5 000 000 g/mol. This extremely large molecular weight has not previously been reported in the literature for the sPS synthesized over heterogeneously supported metallocene catalysts.

The chain length of a polymer is determined by propagation and termination reactions. In sPS polymerization, termination of polymer chain growth occurs by chain transfer reactions: chain transfer to monomer, chain transfer to aluminum components, and β-hydride elimination.[36] Steric hindrance at the polymer-active center in the confined geometry of the nanoscale pores can inhibit chain transfer reactions (chain transfer to monomer and β-hydride elimination). Interestingly, this molecular weight enhancement was also observed in ethylene polymerization with the mesoporous silicas that have pore diameters (3 nm) which are far smaller than the silica nanotubes used in this study.[23,26] Yet, the confined geometry effect in sPS polymerization in SNTR film is quite significant, suggesting that termination of polymer chain growth reaction must have

(35) Huang, B.; Cao, K.; Li, B. G.; Zhu, S. P. *J. Appl. Polym. Sci.* **2004**, *94*, 1449−1455.
(36) Kawabe, M.; Murata, M. *Macromol. Chem. Phys.* **2001**, *202*, 2440−2446.

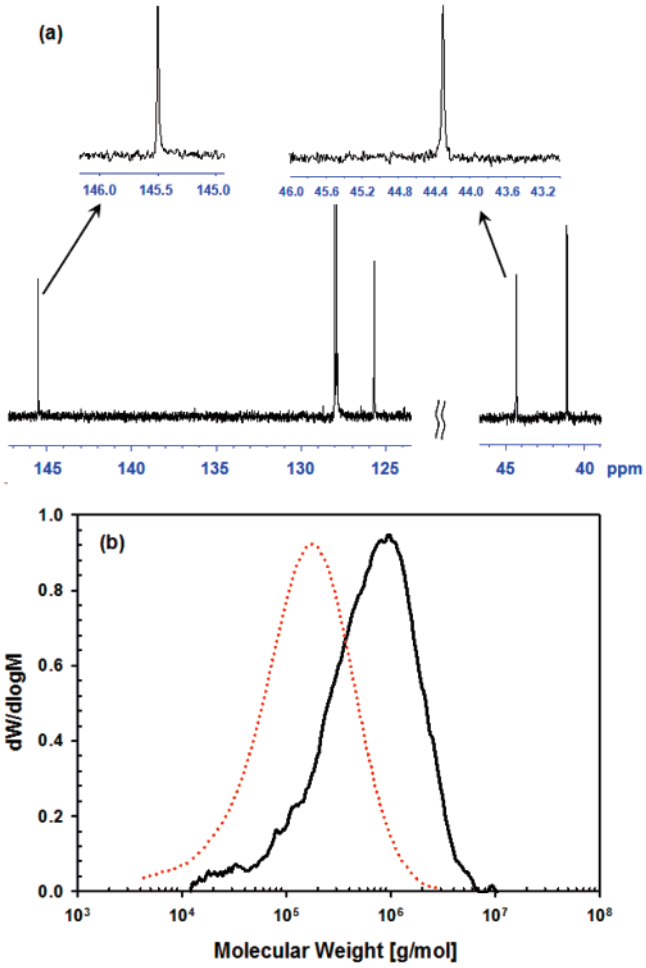

Figure 5. (a) ^{13}C NMR spectrum of sPS nanofibrils. (b) Molecular weight distributions of sPS: SNTR (200 nm), $M_n = 275\,000$ g/mol, $M_w = 928\,000$ g/mol (solid line); silica-supported catalyst, $M_n = 68\,400$ g/mol, $M_w = 221\,000$ g/mol (dotted line).

been greatly inhibited. We found that the sPS in the 60 nm SNTR was extremely difficult to dissolve in trichlorobenzene at 160 °C for several days. GPC analysis of the partially soluble fraction of the polymer sample from the 60 nm SNTR was attempted, but the results were inconsistent.

The sPS polymer synthesized in SNTR was also analyzed by differential scanning calorimetry (DSC). DSC thermograms of three sPS samples synthesized with SNTR, silica-supported catalyst, and homogeneous catalyst are shown in Figure 6. From DSC thermograms, it was found that the first scan melting point was 278.5 °C, which is much higher than the reported value of 270 °C for sPS.[2,12] Such a high melting point of nascent sPS of ultrahigh molecular weight has not been reported in the literature for a nascent sPS synthesized over heterogeneous catalysts. A similar phenomenon of increased crystalline melting point was also observed in polyethylenes synthesized over metallocene catalysts on mesoporous silica fibers or MCM-41.[26] The increase in the melting point has been attributed to formation of extended chain crystals when polyethylene nanofibers are extruded out of the mesopores of 3 nm diameter that prevented the polyethylene chains from folding within the mesopores.[23,26,37−39] In the

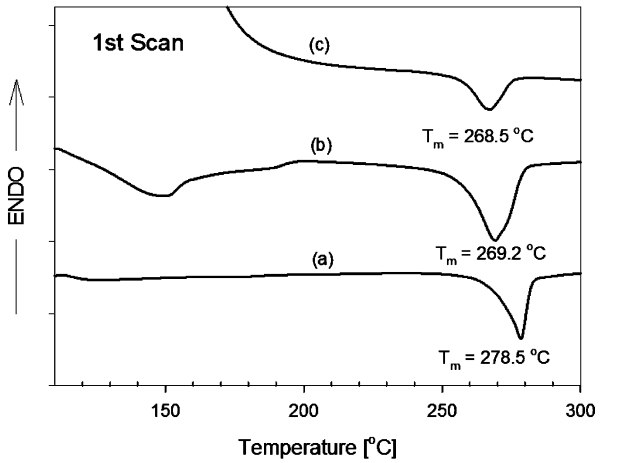

Figure 6. DSC thermograms of sPS: (a) SNTR, (b) silica-supported catalyst, and (c) homogeneous catalyst.

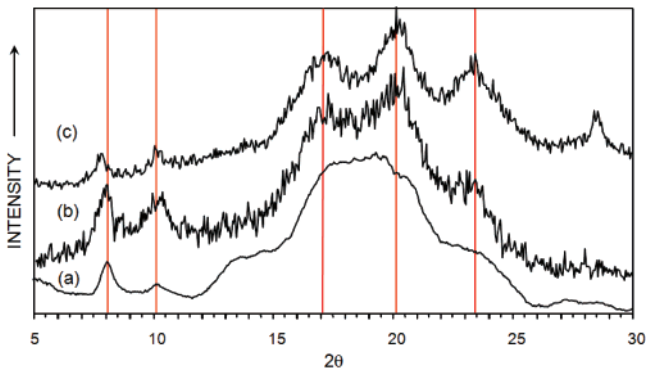

Figure 7. XRD patterns of sPS samples: (a) sPS nanofibrils synthesized in 200 nm SNTR, (b) sPS particles synthesized over silica-supported catalyst, and (c) sPS particle synthesized with homogeneous catalyst.

second scan of the sPS nanofibril sample, the melting point is 270 °C, indicating that the δ-form crystalline structure of the nascent sPS has been transformed to other forms.

The crystalline structure of nascent sPS nanofibrils was analyzed by XRD. SPS is known to have complex crystalline structures (α-, β-, γ-, and δ-form crystals) depending upon the crystallization methods such as solvent casting and thermal annealing.[40−42] Figure 7 shows the XRD patterns of the sPS samples polymerized over homogeneous Cp*Ti$(OCH_3)_3$ catalyst, silica-supported Cp*Ti$(OCH_3)_3$ catalyst, and SNTR. The vertical lines indicate the characteristic peak positions of δ-form sPS crystal ($2\theta \approx 8°$, 10°, 17°, 20°, 23.4°).[43] The sPS samples synthesized over homogeneous and silica-supported catalysts show δ-form crystalline structures. The XRD pattern (a) for the sPS nanofiber sample synthesized in SNTR also shows peaks at 8° and 10°, but the characteristic peaks at $2\theta \approx 17°$, 20°, and 23.4° are not distinctive. The crystalline morphology of sPS is affected by several factors such as complex formation with solvent molecules and the thermal treatment procedure.[44]

(37) Kaminsky, W.; Winkelbach, H. *Top. Catal.* **1999**, *7*, 61−67.
(38) Turunen, J. P. J.; Haukka, M.; Pakkanen, T. T. *J. Appl. Polym. Sci.* **2004**, *93*, 1812−1815.
(39) Dong, X. C.; Wang, L.; Wang, W. Q.; Yu, H. J.; Wang, J. F.; Chen, T.; Zhao, Z. R. *Eur. Polym. J.* **2005**, *41*, 797−803.
(40) Guerra, G.; Vitagliano, V. M.; Derosa, C.; Petraccone, V.; Corradini, P. *Macromolecules* **1990**, *23*, 1539−1544.
(41) Evans, A. M.; Kellar, E. J. C.; Knowles, J.; Galiotis, C.; Carriere, C. J.; Andrews, E. H. *Polym. Eng. Sci.* **1997**, *37*, 153−165.
(42) Tashiro, K.; Ueno, Y.; Yoshioka, A.; Kobayashi, M. *Macromolecules* **2001**, *34*, 310−315.
(43) Rani, D. A.; Yamamoto, Y.; Mohri, S.; Sivakumar, M.; Tsujita, Y.; Yoshimizu, H. *J. Polym. Sci., Part B: Polym. Phys.* **2003**, *41*, 269−273.

The exact reasons for the discrepancies in the XRD patterns at 17°, 20°, and 23.4° are not clear at this point.

For α- or β-form sPS crystals, the crystalline melting point (T_m) tends to increase, albeit slightly, as the thickness of the lamellar is increased.[45−47] XRD analysis indicates that all the sPS samples obtained in our polymerization experiments have the δ-form crystalline structures. When a δ-form crystal is heated above the glass-transition temperature, it is transformed to the γ-form crystal, and above 200 °C, the γ-form is transformed to α-form crystals.[40]

The effect of lamellar thickness (ℓ_c) on the crystalline melting temperature (T_m) can be represented by the Gibbs−Thompson equation[47]

$$T_m = T_m^\circ\left[1 - \frac{2\sigma_e}{\Delta H_f^\circ \ell_c}\right]$$

where T_m° is the equilibrium melting temperature, ΔH_f° is the enthalpy of fusion per unit volume, and σ_e is the fold-surface energy. The Gibbs−Thompson equation indicates that the larger the crystalline lamellar thickness is, the higher the melting temperature becomes. With the parameters of the Gibbs−Thompson equation (T_m° and $\sigma_e/\Delta H_f^\circ$) for α-form sPS crystals,[47] we calculated the lamellar thickness of sPS synthesized in the SNTR. For the sPS with a melting point of 278 °C, the calculated lamellar thickness is 31.6 nm, which is far larger than the lamellar thickness of the sPS with lower melting point (6.33 nm at T_m = 271.6 °C).[47] Since the calculated lamellar thickness for our sPS sample is almost the same as the diameter of a sPS fibril in the 60 nm SNTR, it is thought that crystalline lamellar, if present, would be very hard to see by TEM. Indeed, the high-resolution TEM analysis of the sPS nanofibers inside the SNTR indicates the absence of crystalline lamellar structure (Figure 4b).

In conclusion, the synthesis of syndiotactic polystyrene in a metallocene catalyst-anchored silica nanotube reactor has been investigated. This work presented the first visual evidence of sPS nanofibrils synthesized and extruded out of the SNTR. The 200 nm polymer nanofibril is comprised of intertwined smaller nanofibrils of diameter 30−50 nm. This rope-like cord is composed of even smaller (<10 nm) nanofibrils grown at the catalytic sites on the nanotube walls. It was directly observed through TEM that polymerization in a 60 nm SNTR film produced only a single sPS nanofibril that was 30−35 nm in diameter in each silica nanotube due to the geometrical confinement. The X-ray diffraction and high-temperature GPC analyses indicate the sPS produced in the SNTR is a δ-form crystal polymer that has a ultrahigh molecular weight with a large fraction of 2 000 000−5 000 000 g/mol polymer. It is likely that chain transfer reactions were greatly hindered by the confinement effect of the SNTR. In addition, the ultrahigh molecular weight sPS has a much higher crystalline melting point than those polymerized over silica-supported metallocene catalysts.

Acknowledgment. This work was supported by the National Institute of Standards and Technology, SEF (shared experimental facility), by the UMD-NSF-MRSEC under grant DMR 05-20471 and the University of Maryland. We thank Tim Maugel (Laboratory for Biological Ultrastructure, University of Maryland) for assistance with SEM and TEM.

JA077272N

(44) Gowd, E. B.; Shibayama, N.; Tashiro, K. *Macromolecules* **2006**, *39*, 8412−8418.
(45) Wang, C.; Hsu, Y. C.; Lo, C. F. *Polymer* **2001**, *42*, 8447−8460.
(46) Wang, C.; Cheng, Y. W.; Hsu, Y. C.; Lin, T. L. *J. Polym. Sci., Part B: Polym. Phys.* **2002**, *40*, 1626−1636.
(47) Wang, C.; Chen, C. C.; Hung, C. H.; Lin, K. S. *Polymer* **2004**, *45*, 6681−6689.